Original article

Simultaneous Estimation of Bone Morphology and Fat Fraction Using 1.5 T Magnetic Resonance Imaging

Nobuyuki ARAI[1,2], Koji NAKAYA[1], Kazuhiro ITO[3],
Hiroe MUTO[1], Kanae MATSUURA[1], Koichi SAITO[3]

1) Department of Radiological Technology, Faculty of Health Science, Suzuka University of Medical Science
2) Department of Radiology, Nagoya City University Graduate School of Medical Sciences
3) Department of Rehabilitation, Faculty of Health Science, Suzuka University of Medical Science

Key words: Magnetic resonance imaging, Bone imaging, Fat fraction, In/opposed-phase

Abstract

Intravertebral fat degeneration may be a potential risk factor for bone fractures. Previously, measurements of vertebral morphological changes and fat fraction have been performed separately. However, separate measurements can lead to positioning errors, and with regard to X-ray examinations, an added factor of radiation exposure also exists. Our developed method allows for the simultaneous evaluation of bone morphology and fat fraction using magnetic resonance imaging (MRI), addressing the concerns mentioned above. To obtain a bone image, four in-phase echo images were acquired on a 1.5 T MRI system. We generated a bone image by applying an inversion process to the sum of four images. Additionally, by setting the initial echo time of the multi-echo image to the opposed-phase, the fat fraction was calculated on a pixel-by-pixel basis. Furthermore, a field map was used to correct the inhomogeneity of the magnetic field within the in-plane. Images that enabled the evaluation of bone morphology were obtained from MRI. Using the in-phase images from multi-echo MRI also made it possible to evaluate trabecular bone. Additionally, opposed-phase images were used to calculate fat fraction images. By incorporating the field map into the analysis, obtaining a more accurate image of the fat fraction was possible without magnetic field inhomogeneity. This method can be completed in a single imaging session, with minimal burden on the participant and no positional displacement, in a clinically useful manner.

Introduction

Evaluation of bone morphology, such as in cases of fractures, is commonly performed using X-ray imaging. For example, in the vertebral region, quantitative evaluation is carried out by measuring distances on lateral radiographs of the vertebral bodies. However, this is susceptible to the positioning during imaging, and in cases of early vertebral fractures or occult fractures without morphological changes, it can be difficult to depict them on various X-ray examinations including X-ray computed tomography (CT)[1-4]. Additionally, in osteoporosis, fractures can occur without dependence on bone density, and the importance of bone quality as another factor of bone strength, in addition to bone density, has been pointed out [5, 6].

Evaluation methods for bone morphology include not only the conventional technique of imaging the differences in X-ray absorption that depend on the atomic number of the material, but also magnetic resonance imaging (MRI), which can visualize images based on proton density and its relaxation time. The technique that uses multiple in-phase images acquired using the gradient echo is generally known as the multi-echo method. This is a versatile approach that does not require specialized imaging techniques or analysis programs. Furthermore, MRI is an excellent imaging technique for calculating fat fraction, and studies have been made of the clinical significance of the evaluation of fatty degeneration or infiltration of the liver [7-9], bone marrow [10, 11], heart [12], and muscles [13-15]. Fat fraction is extremely useful clinical information and can be obtained by ultrasound examination; however, MRI can acquire it with high precision using the multi-echo technique [16-18].

Malignant soft tissue tumors such as liposarcoma, which are related to lipid deposition, require a combination of imaging examinations such as CT and MRI for diagnosis, and intravertebral fat degeneration may be a potential risk factor for bone fractures [19, 20]. However, to date, the measurements of vertebral morphological changes and fat fraction have been performed separately. Separate measurements can lead to positioning errors; with regard to X-ray examinations, an added factor of radiation exposure also exists.

This research proposes a method that can simultaneously acquire bone imaging with information on bone morphology and composition, as well as fat fraction imaging, in a single MRI acquisition. The sequence for generating bone images is often performed using a 3.0 T MRI system to improve the signal-to-noise ratio, and three-dimensional (3D) volume imaging is commonly used to enable multi-planar reformatting and acquisition of thin slices [21, 22]. However, the method adopted in this study evaluated the effects using a two-dimensional (2D) gradient-echo sequence using multi-echo, which can be sufficiently set up on a general-purpose MRI system. Our method propose that this is a versatile method that addresses the previously mentioned concerns.

Materials and Methods

We used the fast field echo resembling a CT using restricted echo-spacing (FRACTURE) sequence to obtain a bone image [23]. The evaluation was based on the multi-echo images with in-phase that depends on the magnetic field strength. The number of the in-phase images each echo time (TE) has been reported; however, it has not yet been determined with certainty [21-23]. We applied four TE and generated a bone image by applying an inversion process to the sum of four images. Figure 1 shows the overview of the FRACTURE sequence, which is calculated by fitting the absolute signals into the following equations:

$$S_{\mathrm{sum}}(x,y) = S_0(x,y)\sum_{i=1}^{n} e^{\left(-TE_{\mathrm{IP}_i}/T_2{}^*\right)} \quad (1)$$

$$FRACTURE(x,y) = \left(S(x_{max},y_{max}) + S(x_{min},y_{min})\right) - S_{sum}(x,y) \quad (2)$$

where $S_{sum}(x, y)$ and $S_0(x, y)$ are the signal intensities of summation of each in-phase TE images and the initial signal intensity image, respectively; TE_{IP_i} is each in-phase TE; and $S(x_{max}, y_{max})$ and $S(x_{min}, y_{min})$ are the signal intensities of the maximum and minimum, respectively. Moreover, by setting the initial TE of the multi-echo image to the opposed-phase, the fat fraction $\eta(x, y)$ was calculated on a pixel-by-pixel basis. It is described in the following equations:

$$S_{water}(x,y) = |S_{IP}(x,y) + S_{OP}(x,y)| \quad (3)$$

$$S_{fat}(x,y) = |S_{IP}(x,y) - S_{OP}(x,y)| \quad (4)$$

$$\eta(x,y) = \frac{S_{fat}(x,y)}{S_{water}(x,y) + S_{fat}(x,y)} = \frac{S_{IP}(x,y) - S_{OP}(x,y)}{2S_{IP}(x,y)} \quad (5)$$

where S_{water} and S_{fat} are the signal intensities of the water and the fat, respectively; and $S_{IP}(x, y)$ and $S_{OP}(x, y)$ are the signal intensities of the in-phase image and opposed-phase image, respectively. Furthermore, we used the real component of the complex-valued image to discriminate between fat fraction of 50% and above, and those below 50%. Figure 2 summarizes the process of these image calculations.

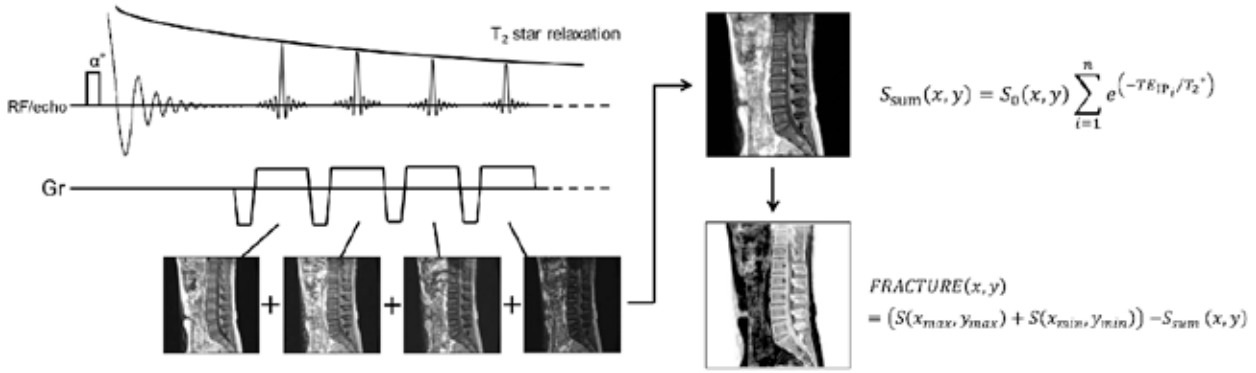

Figure 1

The calculation process of the bone image is as follows. All the echo time (TE) images used in the calculation are at the in-phase timing. Longer TE indicates inclusion of high influence of T_2 relaxation; however, this method sums up all the images and then performs a final black-and-white inversion, so the influence of transverse relaxation is not a problem.

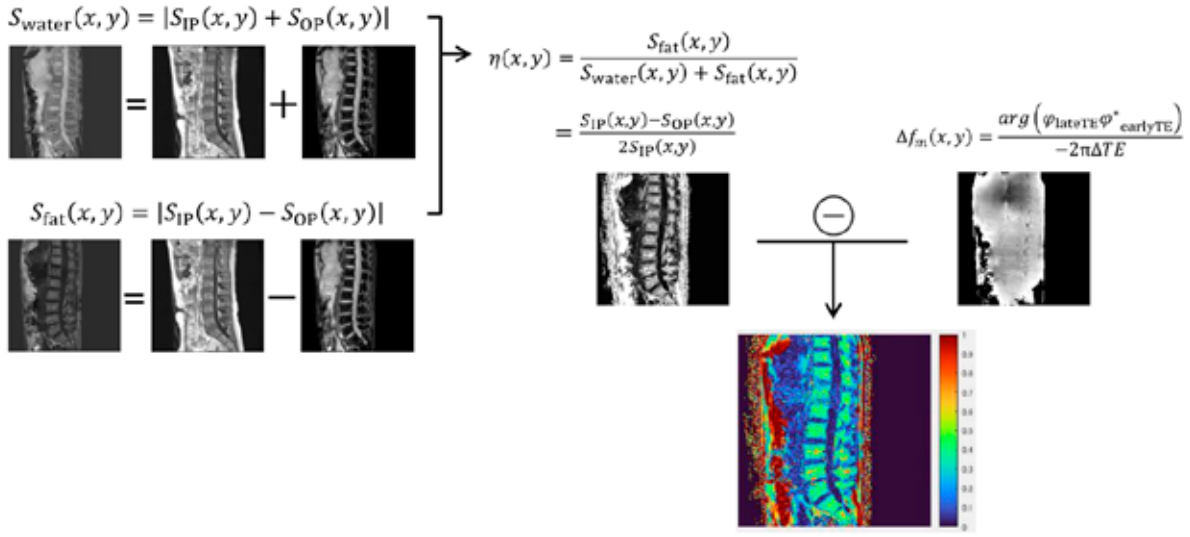

Figure 2

The fat fraction is calculated pixel-by-pixel from the in-phase and opposed-phase images. While the absolute value image alone cannot distinguish between fat fraction below and above 50%, using the real component of the complex-valued image allows accurate representation of fat fraction from 0 to 100%. Furthermore, a field map was created from the phase difference of each TE, and correction for magnetic field inhomogeneity was performed.

Furthermore, a field map $\Delta f_m(x, y)$ was used to correct the inhomogeneity of the magnetic field (B_0) within the in-plane:

$$\Delta f_m(x,y) = \frac{arg\left(\varphi_{\text{lateTE}}\varphi^*_{\text{earlyTE}}\right)}{-2\pi\Delta TE} \quad (6)$$

where φ is the phase difference each TE (* means the complex conjugate of complex number), and ΔTE is the TE difference between early and late TE.

MRI acquisition

All examinations were performed on a 1.5 T MRI system (Echelon Vega, FUJIFILM Healthcare Corporation, Tokyo, Japan) with an eight-channel body matrix coil. To obtain a bone image by applying an inversion process to the sum of four images, we used the following parameters: repetition time (TR), 200 ms; TE, comprising 4 TE, ranged from 4.6–18.4 ms; flip angle, 15°; slice thickness, 5 mm; matrix, 320 × 320; field of view, 320 mm (in-plane resolution, 1.0 × 1.0 mm); parallel imaging factor, 1.0; number of signal averages, 2; receiver bandwidth, 217.4 kHz; and acquisition time, 1 min 46 s. Additionally, to calculate the fat fraction on a pixel-by-pixel basis, the initial TE of the multi-echo image was set to the opposed-phase (i.e., TE, 2.3 ms).

All data were processed with an in-house solution using MATLAB release 2024a (MathWorks Inc., Natick, MA) program and Microsoft Excel 2021 (Microsoft Corporation, Redmond, WA). Moreover, we used ImageJ 1.52 image-processing software (National Institutes of Health, Bethesda, MD) to analyze the images. Since this study proposes a novel image generation method, a bone image was also generated using only the first echo in-phase image as a reference for comparison. Instead of performing statistical analysis, the structural similarity index measure (SSIM)[24] was calculated in the following equations:

$$SSIM(\mathrm{A},\mathrm{B}) = \frac{(2\mu_\mathrm{A}\mu_\mathrm{B} + c_1)(2\sigma_{\mathrm{AB}} + c_2)}{(\mu_\mathrm{A}^2+\mu_\mathrm{B}^2+c_1)+(\sigma_\mathrm{A}^2+\sigma_\mathrm{B}^2+c_2)} \quad (7)$$

where μ_A and μ_B are the average of the reference image and the target image, respectively; σ_A and σ_B are the standard deviation of the reference image and the target image, respectively; σ_{AB} is the sample covariance of the reference image and the target image; and c_1 and c_2 are two variables to stabilize the division with weak denominator, respectively.

Results

The FRACTURE sequence was applied on four in-phase echo images. Using multiple images included T_2 relaxation in accordance with each TE, representing more detailed information about the bone trabeculae (Figure 3a) was possible. The comparison image showing the bone image calculated using only the first echo in-phase image is shown in Figure 3b. The method using the four in-phase echo images showed a significant difference in the trabecular bone compared with the method using only the first echo; however, no significant difference was observed in the cortical bone. Multiple T_2 relaxation information containing images can provide bone images in terms of containing trabecular bone information, compared with images calculated from the first echo alone.

The SSIM between the bone image generated using the four in-phase echo images and that using only the first in-phase echo image is shown in Figure 4. To ensure a more accurate evaluation, the field of view was limited to each lumbar vertebral body, minimizing the inclusion of surrounding organs. The mean SSIM that was calculated across the five vertebral bodies was 0.56644.

To obtain the fat fraction on a pixel-by-pixel whole in-plane images, the in-phase and opposed-phase images were applied. Equation 5 alone was insufficient for accurate calculation, because distinguishing between fat fraction of ≤ 50% and those > 50% was difficult. Next, we used the real component

of the complex-valued image to perform discrimination of fat fraction > 50% (Figure 5a), and solved the conventional problem, as shown in Figure 5b. To compensate for the B_0 inhomogeneity, the field map applied to the in-plane images allowed for the acquisition of more accurate fat fraction.

The multi-echo sequence that was the basis for calculating the FRACTURE image was used to calculate the fat fraction. In other words, the FRACTURE and fat fraction were images that were obtained without any positional mismatch.

Discussion

Evaluation of bone fractures is typically performed using X-ray examination; however, MRI can also be used to visualize bones, and its usefulness has been reported [21-23]. MRI is also an excellent examination for evaluating fat fraction [7, 14, 16-18]. The relationship between bone lesions and fat fraction has been reported [17, 25, 26]. Bone density tests (e.g., dual energy X-ray absorptiometry) reflect bone mineral content; however, in bones with high fat content, the bone mineral content may be underestimated [26]. This suggests that

Figure 3
Calculation of bone images requires in-phase images; however, the calculation image using multiple TE (a) and only the TE of the first echo (b) are shown. The image with the application of multiple TE can evidently better depict the fine structure of the bone and the information of the bone trabeculae.

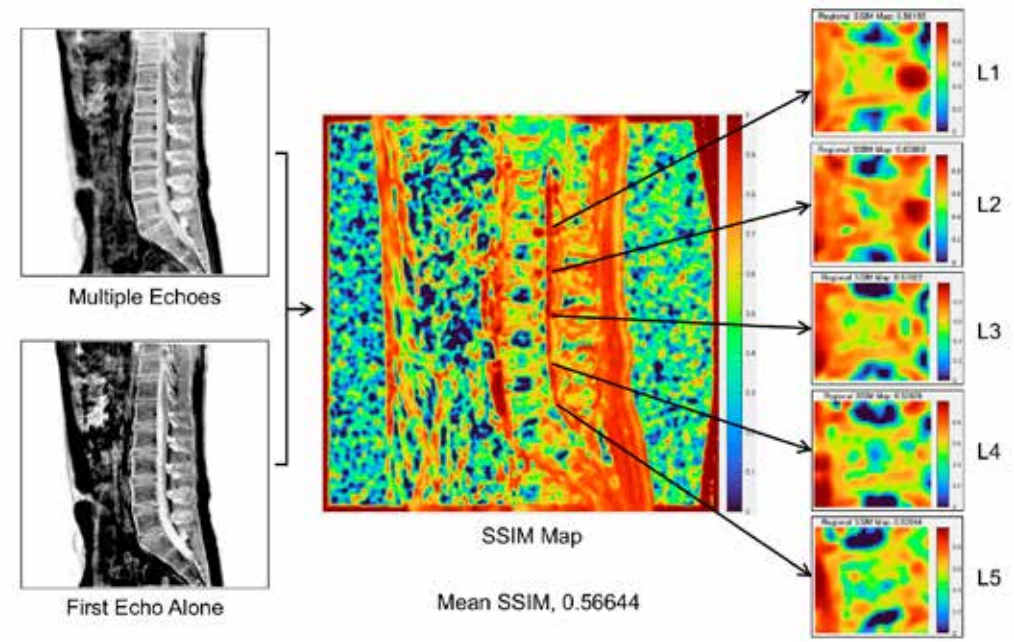

Figure 4
The SSIM was between the bone image generated using the four in-phase echo images and that using only the first in-phase echo image. The mean SSIM was calculated across the five vertebral bodies.

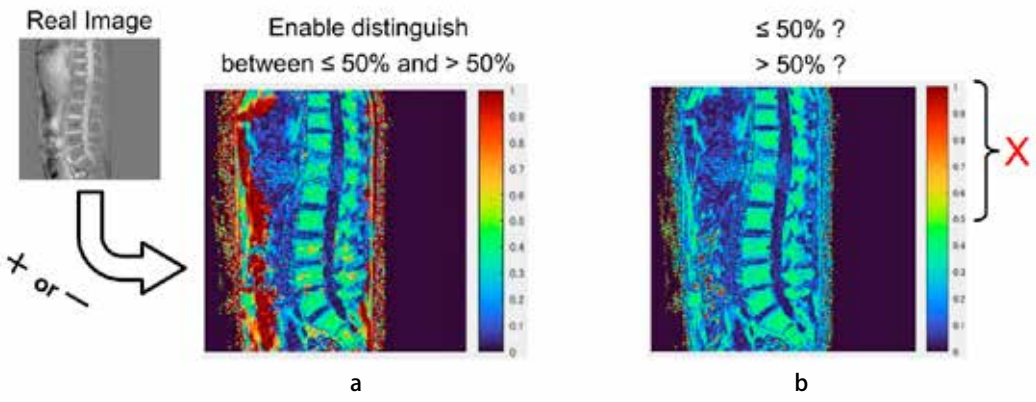

Figure 5

The real component of the complex-valued image applied to create a fat fraction image (a), and a fat fraction image calculated solely from the magnitude MR image (b). Using the real component, distinguishing between fat fraction of ≤ 50% and those > 50% was possible. However, when calculating solely from the absolute value image, the fat fraction > 50% would appear to have the same signal fat fraction of ≤ 50%.

evaluating the composition of the bone and its fat fraction is clinically significant. When these cases are diagnosed, we require a combination of imaging examinations such as X-ray examinations and MRI. In this study, we developed a method that can simultaneously acquire bone images and fat fraction in one scan using multi-gradient echo sequence.

The FRACTURE sequence that has been reported is generally calculated from multiple in-phase images. In this study, 4 TE were adopted for verification. However, these TE must be set to the in-phase, which is not the shortest, and in the case of a general-purpose MRI system with a static magnetic field strength of 1.5 T, the later TE may be extended, resulting in a possible extension of TR as well. Therefore, we attempted to calculate bone images using only the first echo in order to resolve the concern of time extension. For the signal-to-noise ratio, the bone image was calculated by adding the first echo images in the same number. As a result, the bone images using only the first echo lacked information on the bone trabeculae, and the method using multiple different TE was similar contrast to that of X-ray CT images. The SSIM values for each lumbar vertebral body were substantially lower than 1, which is the value for identical images. Specifically, the cortical bone showed SSIM values close to 1, whereas the trabecular bone exhibited lower values. This is because the characteristics of the FRACTURE sequence calculation method. Specifically, this technique uses a black-and-white inversion process at the end of the image operation. Consequently, when the same image is added, the signal values are simply summed, which tends to result in a low-signal final image. Per the above discussion, we can conclude that images that enable the evaluation of bone morphology similar contrast to X-ray CT were obtained from MRI; using the in-phase images from multi-echo MRI also made it possible to evaluate trabecular bone. On the other hand, if the evaluation is only for the structural assessment of the bone, such as a fracture, the bone image obtained from the first echo alone may be sufficient. In that case, the acquisition time would not be prolonged and the derivation would also be simpler.

Additionally, opposed-phase images that were obtained in conjunction with the in-phase by the multi-echo simultaneously were used to calculate fat fraction images. We adopted the two-point type Dixon method, which can also be applied to the conventional MR system. This is because the multi-point type, which is said to have high accuracy, often requires optional special programs and lacks versatility. Additionally, the slight decrease in the accuracy

of fat fraction is not considered very important in the diagnosis. The precision degradation caused by B_0 inhomogeneity is a more fundamental issue underlying MRI than the accuracy differences between two-point and multi-point measurement methods [27, 28]. Therefore, we performed B_0 inhomogeneity correction using the field map on a pixel-by-pixel basis. By incorporating the field map into the analysis, obtaining a more accurate image of the fat fraction without B_0 inhomogeneity was possible.

The calculation of fat fraction using the two-point Dixon method is simple and can be easily implemented even on conventional MRI systems. However, simply using the intensity information from in-phase and opposed-phase images makes it difficult to distinguish between fat fractions below and above 50%. This is because even if a difference in the absolute magnitude of the magnetic moments of the protons that make up water and fat on a per-pixel basis is noted, all of those absolute values are expressed as signal intensity. To solve this problem, we used the real-image component of the MRI complex data. The signal intensity in an MRI image is not only proportional to the water and fat content on a per-pixel basis, but it also depends on the composite vector arising from the phase difference between the resonance frequencies of the protons that make up water and fat. Therefore, we determined the sign of each pixel in the real component, and classified pixels with positive values as having a fat fraction of ≤ 50%, whereas pixels with negative values were considered to have a fat fraction > 50%. Fat fraction imaging can be calculated from images obtained by FRACTURE sequence acquisition, which is an excellent method that imposes little physical and economic burden on the patient.

The proposed method that allows for both bone morphology imaging and fat content evaluation in a single MRI acquisition is considered highly useful. However, we recognize the following limitations. This research is focused on methods for acquiring images. Therefore, the visualization of some lesions has not been investigated. In the future, we would like to conduct our method in a variety of cases and explore the clinical utility of this approach. Another limitation is that the study was unable to evaluate the fat fraction using established fat mass measurements. The current research involved B_0 inhomogeneity correction; however, the fat fraction is calculated from a two-point TE method, so the measurement accuracy needs to be verified. If these limitations are resolved, this method would become a clinically useful imaging tool and contribute to reducing the burden on patients.

Conclusion

This study proposed a useful method that can acquire the morphological information of bone and fine structure of trabeculae. Acquiring an image of the fat fraction with the correction of B_0 inhomogeneity simultaneously is possible, with minimal burden on the patient and no positional displacement, in a clinically useful manner. The proposed technique, which can provide two clinically useful pieces of information in a single MRI acquisition, is superior in simultaneous evaluation due to the lack of positional misalignment and has great potential to reduce the physical and economic burden on the patient.

Acknowledgements

This study was funded by Japan Society for the Promotion of Science (JSPS) KAKENHI Grant Number JP20K16767.

References

1）Li J, She B, He M, Yuan C,Li N. Advances in imaging examination of bone density and bone quality. Endokrynol Pol. 2025; 76: 29-39.

2）Wang F, Zheng L, Theopold J, Schleifenbaum S, Heyde CE, Osterhoff G. Methods for bone quality assessment in human bone tissue: a systematic review. J Orthop Surg

Res. 2022; 17: 174.

3）Safir O, Lin C, Kosashvili Y, Mayne IP, Gross AE,Backstein D. Limitations of conventional radiographs in the assessment of acetabular defects following total hip arthroplasty. Can J Surg. 2012; 55: 401-407.

4）Donnelly E. Methods for assessing bone quality: a review. Clin Orthop Relat Res. 2011; 469: 2128-2138.

5）Gold LS, Cody RF, Jr., Tan WK, Marcum ZA, Meier EN, Sherman KJ, et al. Osteoporosis identification among previously undiagnosed individuals with vertebral fractures. Osteoporos Int. 2022; 33: 1925-1935.

6）Lenchik L, Rogers LF, Delmas PD, Genant HK. Diagnosis of osteoporotic vertebral fractures: importance of recognition and description by radiologists. Am J Roentgenol. 2004; 183: 949-958.

7）Fetzer DT, Pierce TT, Robbin ML, Cloutier G, Mufti A, Hall TJ, et al. US Quantification of Liver Fat: Past, Present, and Future. Radiographics. 2023; 43: e220178.

8）Igarashi H, Shigiyama F, Wakui N, Nagai H, Shibuya K, Shiraga N, et al. Whole hepatic lipid volume quantification and color mapping by multi-slice and multi-point magnetic resonance imaging. Hepatol Res. 2019; 49: 1374-1385.

9）Reeder SB,Sirlin CB. Quantification of liver fat with magnetic resonance imaging. Magn Reson Imaging Clin N Am. 2010; 18: 337-357, ix.

10）Li X, Schwartz AV. MRI Assessment of Bone Marrow Composition in Osteoporosis. Curr Osteoporos Rep. 2020; 18: 57-66.

11）Cordes C, Baum T, Dieckmeyer M, Ruschke S, Diefenbach MN, Hauner H, et al. MR-Based Assessment of Bone Marrow Fat in Osteoporosis, Diabetes, and Obesity. Front Endocrinol (Lausanne). 2016; 7: 74.

12）Homsi R, Meier-Schroers M, Gieseke J, Dabir D, Luetkens JA, Kuetting DL, et al. 3D-Dixon MRI based volumetry of peri- and epicardial fat. Int J Cardiovasc Imaging. 2016; 32: 291-299.

13）Huber FA, Del Grande F, Rizzo S, Guglielmi G, Guggenberger R. MRI in the assessment of adipose tissues and muscle composition: how to use it. Quant Imaging Med Surg. 2020; 10: 1636-1649.

14）Faron A, Sprinkart AM, Kuetting DLR, Feisst A, Isaak A, Endler C, et al. Body composition analysis using CT and MRI: intra-individual intermodal comparison of muscle mass and myosteatosis. Sci Rep. 2020; 10: 11765.

15）Burakiewicz J, Sinclair CDJ, Fischer D, Walter GA, Kan HE,Hollingsworth KG. Quantifying fat replacement of muscle by quantitative MRI in muscular dystrophy. J Neurol. 2017; 264: 2053-2067.

16）Qi R, Lu L, He T, Zhang L, Lin Y, Bao L. Comparing ultrasound-derived fat fraction and MRI-PDFF for quantifying hepatic steatosis: a real-world prospective study. Eur Radiol. 2025; 35: 2580-2588.

17）Beyer C, Hutton C, Andersson A, Imajo K, Nakajima A, Kiker D, et al. Comparison between magnetic resonance and ultrasound-derived indicators of hepatic steatosis in a pooled NAFLD cohort. PLoS One. 2021; 16: e0249491.

18）Kramer H, Pickhardt PJ, Kliewer MA, Hernando D, Chen GH, Zagzebski JA, et al. Accuracy of Liver Fat Quantification With Advanced CT, MRI, and Ultrasound Techniques: Prospective Comparison With MR Spectroscopy. Am J Roentgenol. 2017; 208: 92-100.

19）Zoulakis M, Axelsson KF, Litsne H, Johansson L, Lorentzon M. Bone Marrow Adiposity Assessed by HRpQCT Is Related to Fracture Risk and Bone Mineral Density in Older Swedish Women. J Clin Endocrinol Metab. 2025;

20）Schwartz AV. Marrow fat and bone: review of clinical findings. Front Endocrinol (Lausanne). 2015; 6: 40.

21）Tsuchiya K, Gomyo M, Katase S, Hiraoka S,Tateishi H. Magnetic resonance bone imaging: applications to vertebral lesions. Jpn J Radiol. 2023; 41: 1173-1185.

22）Naraghi A,White LM. Three-dimensional MRI of the musculoskeletal system. AJR Am J Roentgenol. 2012; 199: W283-293.

23）Johnson B, Alizai H, Dempsey M. Fast field echo resembling a CT using restricted echo-spacing (FRACTURE): a novel MRI technique with superior bone contrast. Skeletal Radiol. 2021; 50: 1705-1713.

24）Wang Z, Bovik AC, Sheikh HR, Simoncelli EP. Image quality assessment: from error visibility to structural similarity. IEEE Trans Image Process. 2004; 13: 600-612.

25）Yeung DK, Griffith JF, Antonio GE, Lee FK, Woo J,Leung PC. Osteoporosis is associated with increased marrow fat content and decreased marrow fat unsaturation: a proton MR spectroscopy study. J Magn Reson Imaging. 2005; 22: 279-285.

26）Salamone LM, Fuerst T, Visser M, Kern M, Lang T, Dockrell M, et al. Measurement of fat mass using DEXA: a validation study in elderly adults. J Appl Physiol. 2000; 89: 345-352.

27）Bray TJ, Chouhan MD, Punwani S, Bainbridge A, Hall-Craggs MA. Fat fraction mapping using magnetic resonance imaging: insight into pathophysiology. Br J Radiol. 2018; 91: 20170344.

28）Delfaut EM, Beltran J, Johnson G, Rousseau J, Marchandise X, Cotten A. Fat suppression in MR imaging: techniques and pitfalls. Radiographics. 1999; 19: 373-382.

— プロフィール ——————————————

荒井　信行　鈴鹿医療科学大学保健衛生学部放射線技術科学科・助教　博士（保健学）

〔経歴〕2005 年国際医療福祉大学保健学部放射線情報科学科卒業，2006 年名古屋市立大学病院中央放射線部（現 診療技術部放射線技術科），2007 年金沢大学大学院医学系研究科保健学専攻博士前期課程修了，2018 年名古屋市立大学医学研究科放射線医学分野研究員，2020 年より現職，2022 年金沢大学大学院医薬保健学総合研究科保健学専攻博士後期課程修了。〔専門〕放射線科学，磁気共鳴医学。

中舎　幸司　鈴鹿医療科学大学保健衛生学部放射線技術科学科・准教授　博士（保健学）

〔経歴〕2005 年鈴鹿医療科学大学保健衛生学部放射線技術科学科卒業，2005 年洛和会音羽病院，2005 年国立病院機構京都医療センター，2007 年国立循環器病研究センター，2015 年徳島大学大学院保健科学教育部保健学専攻医用情報科学領域博士前期課程修了（保健学修士），2015 年鈴鹿医療科学大学保健衛生学部放射線技術科学科助教，2018 年金沢大学大学院医薬保健学総合研究科保健学専攻博士後期課程修了（保健学博士），2021 年より現職。〔専門〕放射線科学。

伊藤　和寛　鈴鹿医療科学大学保健衛生学部リハビリテーション学科理学療法学専攻・助教　博士（スポーツ科学）

〔経歴〕2003 年吉備国際大学保健科学部理学療法学科卒業，2003 年医療法人恒仁会近江温泉病院勤務，2018 年より現職，2025 年大阪体育大学大学院スポーツ科学研究科スポーツ科学専攻博士後期課程修了。〔専門〕神経系理学療法，バイオメカニクス，トレーニング科学。

武藤　裕衣　鈴鹿医療科学大学保健衛生学部放射線技術科学科・教授　博士（保健衛生学）

〔経歴〕1995 年鈴鹿医療科学技術大学保健衛生学部放射線技術科学科卒業（保健衛生学学士），2002 年鈴鹿医療科学大学大学院保健衛生学研究科博士課程（後期）課程修了博士（保健衛生学），1995 年鈴鹿医療科学技術大学保健衛生学部放射線技術科学科助手，2010 年鈴鹿医療科学大学保健衛生学部放射線技術科学科准教授，2019 年より現職。〔専門〕診療放射線技師教育，医療画像技術学，医療被曝。

松浦　佳苗　鈴鹿医療科学大学保健衛生学部放射線技術科学科・教授　博士（保健学）

〔経歴〕2003 年鈴鹿医療科学大学大学院保健衛生学研究科医療画像情報学専攻修士課程修了，2008 年鈴鹿医療科学大学保健衛生学部放射線技術科学科助教，2013 年鈴鹿医療科学大学保健衛生学部放射線技術科学科准教授，2022 年金沢大学大学院医薬保健学総合研究科博士課程修了，2025 年より現職。〔専門〕放射線科学，画像情報処理，教育工学。

齋藤　恒一　鈴鹿医療科学大学保健衛生学部リハビリテーション学科・助教　修士（保健学）

〔経歴〕2000 年吉備国際大学保健科学部理学療法学科卒業，2009 年岡山大学保健学研究科博士前期課程修了（修士），2010 年鈴鹿医療科学大学保健衛生学部理学療法学科助手，2018 年より現職，2022 年大阪体育大学スポーツ科学研究科博士後期課程単位取得後満期退学。〔専門〕リハビリテーション科学，災害支援，緩和ケア領域の理学療法。

1.5 T MRI を用いた骨形態と脂肪含有率の同時描出

荒井　信行[1, 2)]，中舎　幸司[1)]，伊藤　和寛[3)]，
武藤　裕衣[1)]，松浦　佳苗[1)]，齋藤　恒一[3)]

1）鈴鹿医療科学大学　保健衛生学部　放射線技術科学科
2）名古屋市立大学　医学研究科　放射線医学分野
3）鈴鹿医療科学大学　保健衛生学部　リハビリテーション学科

キーワード：　Magnetic resonance imaging, Bone imaging, Fat fraction, In/opposed-phase

要　旨

椎体の脂肪変性は，骨折の潜在的なリスク因子となる可能性がある。これまで椎体の形態変化と脂肪含有率の測定は別々に取得されていた。しかし，個々の測定は位置ずれを引き起こす可能性があり，また X 線検査の場合は放射線被曝の懸念もある。本研究で開発した手法は，MRI を用いて骨形態と脂肪含有率を同時に描出し，上述の課題を解決するものである。1.5T MRI 装置を使用し，4 つの同位相エコーの合成画像に反転処理を適用して骨画像を取得し，骨形態や海綿骨の評価が可能となった。さらに，第 1 エコーの逆位相画像を用いて脂肪含有率を算出し，その際面内の磁場不均一性を補正するために field map を適用し，より正確な脂肪含有率画像を取得することが可能となった。この手法は，一度の撮像で複数の臨床情報を取得することができ，かつ被検者の負担が最小限となるため，臨床的に有用となることが期待できる。